Mass Flow through Solid ^{3}He in the bcc Phase

Zhi Gang Cheng[1,2,3,*] and John Beamish[2,†]
[1]Beijing National Laboratory for Condensed Matter Physics, Institute of Physics, Chinese Academy of Sciences, Beijing, 100190, China
[2]Department of Physics, University of Alberta, Edmonton, Alberta, T6G 2E1, Canada
[3]Songshan Lake Materials Laboratory, Dongguan, Guangdong, 523808, China

(Received 10 September 2018; revised manuscript received 23 October 2018; published 29 November 2018)

A number of experiments have shown that mass can be transported through solid ^{4}He at temperatures as low as 16 mK, with features that suggest superflow. But the nature of this flow remains unclear. The Fermi isotope ^{3}He provides the possibility of a direct comparison to a solid in which quantum effects are even more important but superfluidity is not expected. We have made flow measurements on high purity bcc ^{3}He, using the same cell in which we observed a superfluidlike response in hcp ^{4}He when pressure differences were applied. We observed flow but, in marked contrast to ^{4}He, it decreased monotonically with temperature. Near melting, the flow was thermally activated with an energy of 0.85 K, but some flow remained even at 30 mK. The flow rates in the solid were essentially constant below 100 mK, even in low density samples that remelted at low temperatures. The very different behaviors of solid ^{3}He and ^{4}He support the interpretation of superflow in ^{4}He. Although such superflow is not possible in ^{3}He, the temperature-independent flow below 100 mK indicates that the flow in this regime also has a quantum origin. The flow must involve defects and, based on the magnitude of the flow and comparisons to other experiments, we conclude that in both the thermal and the quantum regimes the flow involves motion of dislocations via thermally activated or tunneling motion of kinks.

DOI: 10.1103/PhysRevLett.121.225304

Solid helium is a uniquely quantum material with unusual features at low temperatures. The most spectacular prediction is of supersolidity in hcp ^{4}He [1–3]. The first experimental claim of supersolidity involved torsional oscillator experiments [4,5] in which the oscillator's period decrease below 200 mK was interpreted as decoupling of supersolid mass. Most such observations are now understood as effects of anomalous elastic effects in solid ^{4}He [6–8], although a few recent torsional oscillator experiments [9–11] still show hints of possible supersolidity. Superfluidlike mass flow has also been observed in dc mass flow experiments. The pioneering experiments involved a solid ^{4}He sample sandwiched between two "superfluid leads" of liquid ^{4}He confined in porous Vycor glass. Applying a pressure difference via these leads created a flow through a solid ^{4}He channel [12,13]. This flow occurred only below 600 mK and the rate increased as the sample was cooled, confirming that it was not associated with a thermally activated process. The flow was abruptly suppressed below a temperature $T_d \approx 100$ mK, which depended on x_3, the ^{3}He impurity concentration ($x_3 \approx 120$ ppm in commercial ^{4}He gas). It was interpreted in terms of superflow along the cores of a dislocation network, modeled as one-dimensional (1D) Luttinger liquids, and the suppression at T_d was attributed to ^{3}He impurities binding to dislocations and disrupting the flow. However, estimates for the ^{3}He concentration needed to block the flow in a network of 1D dislocations give $x_3 \approx 10^{-9}$, about 10^4 times lower than the observations [13]. A more recent experiment [14] with similar geometry, but with a much thinner (8 μm) solid region between the Vycor leads, exhibited similar behavior except that flow suppression was observed only for $x_3 \geq 6\%$, i.e., the concentration at which phase separation occurs in liquid ^{3}He – ^{4}He mixtures. The difference was attributed to the lack of dislocation intersections in the 8 μm solid region, suggesting that ^{3}He impurities block the flow when they concentrate at nodes of the network, but in large crystals blocking at nodes would require ^{3}He concentrations even smaller than $x_3 = 10^{-9}$.

We recently showed that similar mass flow can also be generated without superfluid leads, by applying mechanical compression directly to solid ^{4}He [15,16]. As in the other experiments, the flow began at 600 mK, increased as the temperature decreased, and was suppressed at a similar T_d. The path for this superfluidlike flow is still unclear. Comparing the dependence of T_d on x_3 in the different experimental geometries suggests that the mass flow occurs in two-dimensional (2D) channels along solid surfaces or grain boundaries. However, the flow does not show the characteristic Kosterlitz-Thouless temperature seen in 2D ^{4}He films [17].

Quantum effects are even larger in ^{3}He, with its lighter mass and larger zero-point motion. However, ^{3}He is a fermion, so superfluidity requires pairing [18,19] and occurs only below 2.4 mK. In solid ^{3}He, magnetic ordered phases onset in a similar temperature range but our experiments were done above 30 mK, where body-centered cubic (bcc) ^{3}He is in the paramagnetic phase. Dislocations exist in solid ^{3}He [20,21], but will not exhibit the superfluid properties predicted for dislocations in ^{4}He. However, the solid's large zero-point energy makes defects like vacancies and dislocations very mobile so they may contribute to mass transport at low temperatures. Experiments with ^{3}He can provide a potential touchstone: a direct comparison between the Bose solid ^{4}He, where superfluidlike flow was observed, and the Fermi solid ^{3}He, for which superfluid flow paths are not expected.

In this Letter, we present measurements of mass flow in bcc ^{3}He using the *same* cell and technique with which we previously observed superfluidlike low temperature flow in hcp ^{4}He [16]. Polycrystalline solid ^{3}He samples were grown using the same constant volume blocked-capillary method as was used for the ^{4}He experiments. We used high purity ^{3}He gas (^{4}He concentration $x_4 = 1.35$ ppm). Since mass flow in solid ^{4}He has been observed only near its melting pressure [13–16], we prepared ^{3}He crystals in the low pressure bcc phase. Three samples were studied, starting with liquid ^{3}He at 46.0, 41.7, and 39.0 bar, giving pressures when the samples were completely frozen of 36.4, 32.6, and 30.6 bar, respectively. The highest pressure sample remained solid at all temperatures below its melting point $T_M = 870$ mK. For the two lower pressure samples, which were prepared by slower cooling, freezing was complete at $T_M = 660$ and 520 mK, respectively. Because the ^{3}He melting pressure has a minimum at 319 mK, and rises to ~34 bar close to 0 K [22], these samples partially melted at lower temperatures, beginning at $T_{LM} = 51$ and 140 mK, respectively. Pressure differences were generated along the cylindrical helium channel by applying either an ac or a dc voltage to a piezoelectric actuator. This displaced the diaphragm and compressed the solid at one end of the channel. A capacitive sensor measured the resulting pressure response $P(t)$ at the opposite end. The rate of pressure change $\dot{P}(t)$ was a measure of the resulting flow rate. At high temperatures, where the pressure responded within seconds, we used an ac mode, applying a sinusoidal voltage $V(t) = V_0 \cos(2\pi f t)$ with amplitude $V_0 = 50$ V and frequency $f = 0.02$ Hz. A lock-in amplifier was used to measure the pressure response, $\Delta P(t) = \Delta P_{\rm ac} \cos(2\pi f t + \phi)$, where $\Delta P_{\rm ac} \propto \partial \Delta P(t)/\partial t$ is a measure of the rate of pressure change. When the flow rate was low, we used the dc mode described later.

Figure 1(a) compares the temperature dependence of $\Delta P_{\rm ac}$ of the 36.4 bar ^{3}He sample to that of a 26.5 bar hcp ^{4}He crystal [16]. The ^{4}He crystal was prepared with extremely high purity ($x_3 \approx 5 \times 10^{-12}$) and no suppression at low temperature was observed. In ^{3}He, $\Delta P_{\rm ac}$ decreased monotonically as the temperature was lowered from 0.8 to 0.3 K, then remained constant, with no sign of an increase at temperatures down to 30 mK. Below 300 mK the flow was too slow to be detected by this ac technique and a dc method had to be used, as discussed below. The opposite behavior was seen in ^{4}He, where flow appeared below 600 mK and increased monotonically down to the lowest temperature of 16 mK. The marked contrast between the flow in crystals of the two isotopes, ^{3}He and ^{4}He, is further evidence that the low temperature flow in solid ^{4}He involves some form of superfluidity.

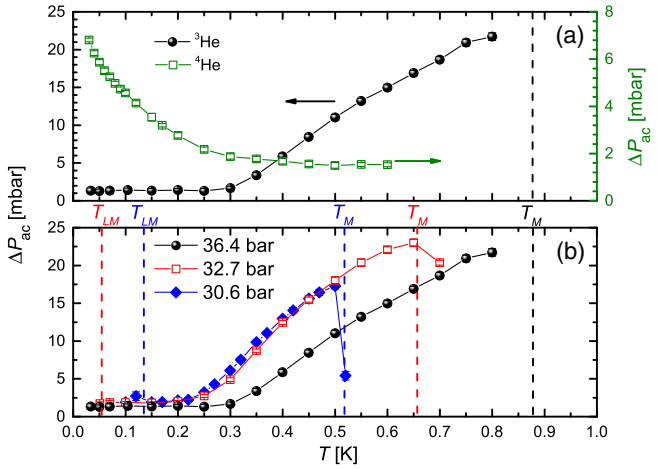

FIG. 1. (a) Temperature dependence of ac pressure response $\Delta P_{\rm ac}$ for bcc ^{3}He sample at 36.4 bar (left axis) and hcp ^{4}He sample reported in Ref. [16] (right axis). (b) Temperature dependence of $\Delta P_{\rm ac}$ for solid ^{3}He at 30.6, 32.7, and 36.4 bar. Dashed lines indicate the melting (and remelting) temperatures for samples represented by the data of the same colors.

ΔP_{ac} is composed of an elastic response and the mass flow signal. The first contribution just reflects the elastic deformation at the pressure sensor due to the compression at the opposite end. Since the elastic constants of helium depend weakly on temperature and the elastic response is much faster than 0.02 Hz, this contribution is essentially constant and in phase with the applied compression ($\phi = 0$, see Supplemental Material [22]). It dominates the flow above 0.5 K in solid ^{4}He, and below 0.3 K in solid ^{3}He. The elastic ΔP_{ac} is similar in ^{3}He and ^{4}He (~1.6 mbar for $V_0 = 50$ V), as expected because elastic constants of these two isotopes are similar. In ^{3}He, $\Delta P_{\rm ac}$ starts to increase above ~0.3 K, as mass flow becomes significant. The flow increases monotonically up to the melting temperature T_M. On the other hand, $\Delta P_{\rm ac}$ for ^{4}He monotonically increases as temperature is reduced below 0.5 K as the superfluidity becomes more obvious.

Figure 1(b) compares the responses of ^{3}He samples with different densities. The two lower pressure samples (32.7 and 30.6 bar) remelted when cooled below T_{LM} (51

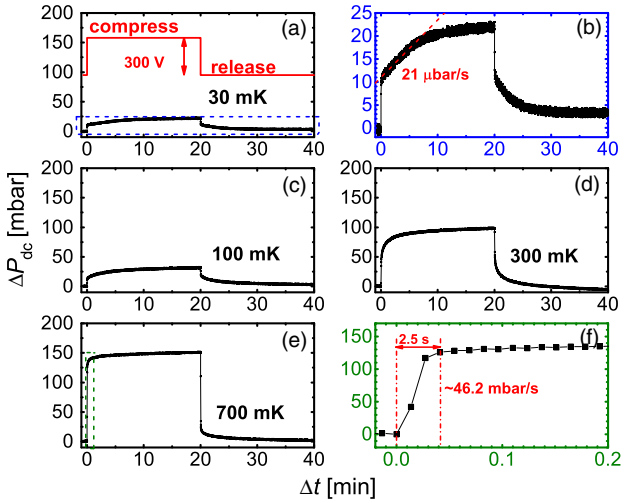

FIG. 2. (a),(c),(d),(e) dc pressure responses at 30, 100, 300, and 700 mK when one end is compressed and then released with the profile indicated by the red solid line in (a). (b),(f) Expanded views of the responses at 30 and 700 mK within the dashed frames shown in (a) and (e). Flow rates are estimated from the linear fit (red dashed line) at 30 mK and from the pressure rise over 2.5 s after subtracting the elastic pressure jump at 700 mK.

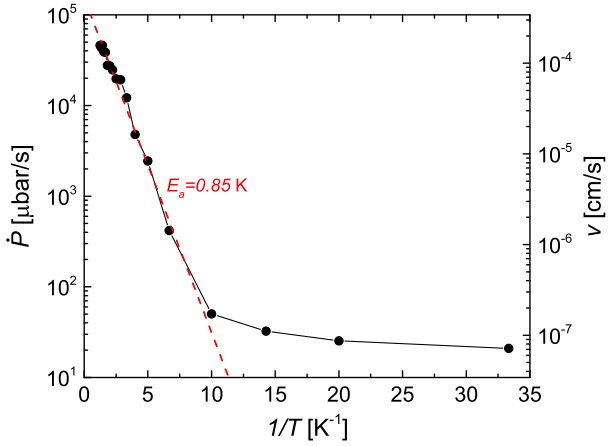

FIG. 3. Arrhenius plot of flow rate $\dot{P}$ and estimated flow speed v against inverse temperature $1/T$.

and 140 mK, respectively). The lower and upper melting transitions reflect entropy differences between liquid and solid ^{3}He, but both are first order transitions so no precursors to melting are seen. The behavior of the low pressure samples is qualitatively similar to that of the first sample, but the flow starts to increase at lower temperatures (around 0.2 K), suggesting that the energies associated with this thermal flow are smaller. This could be due to the smaller vacancy energies in the lower density samples. The flow could also reflect the samples' growth histories, which can affect defect densities. For these samples we have included a data point just above T_M, which shows the sudden drop in the pressure response when even a small amount of liquid is present.

Measurements in ac mode are insensitive to slow mass flow that does not generate a significant pressure response within the time period of $(2\pi f)^{-1}$. To clarify the behavior in ^{3}He, we switched to a dc technique to resolve the flow at temperatures below 300 mK. A voltage of 300 V was applied to compress the helium at one end by about ~ 1 μm, and then removed 20 min later to reverse the deformation. Figure 2 shows the dc pressure response at different temperatures. Compression produces an immediate elastic response [$\sim$11 mbar, most obvious in the 30 mK data in Fig. 2(b)]. This jump is $\sim$6 times larger than the ac elastic response in Fig. 1, as expected given the different dc and ac voltages (300 and 50 V, respectively). Even at the lowest temperature, the elastic jump was followed by a gradual pressure increase, the signature of mass flow. At 30 mK, the pressure rose at a nearly constant rate $\dot{P} \sim 21$ μbar/s for about 5 min, then began to saturate, with a total increase of $\sim$13 mbar in addition to the initial elastic jump in 20 min. When the compression was released, the response was similar but inverted. With increasing temperature, the flow rate and the total pressure change both increased, consistent with the ac data of Fig. 1. By 700 mK [Fig. 2(f)], the dc pressure rise occurred within a few seconds and saturated at $\sim$150 mbar, about 60% of the change expected for full hydrostatic pressure relaxation [22]. At this temperature, the elastic jump cannot be distinguished from the rapid pressure change due to mass flow. We can estimate the flow rate by subtracting 11 mbar from the total pressure change, giving a flow rate of 46.2 mbar/s during the first 2.5 s, more than 2000 times higher than at 30 mK.

Flow rates calculated in this way are shown in the Arrhenius plot of Fig. 3. Above 100 mK the flow is thermally activated with an activation energy $E_a \approx 0.85$ K. Below 100 mK, the flow deviates from this behavior and appears to approach a constant value of $\sim$20 μbar/s. The weak temperature dependence below 50 mK, appears to be approaching to a constant flow rate, and is not consistent with activation energies larger than 16 mK, i.e., well below the energies of known defects in solid helium. Thus it suggests a nonthermal, quantum contribution to the flow.

Activated flow has been seen above 0.7 K in bulk ^{4}He ($T_M = 1.6$ K) [15] and near the melting temperature in ^{4}He confined in 25 μm channels ($T_M = 2.05$ K) [29]. Zhuchkov *et al.* [30] used a very sensitive technique in which flow was determined from the displacement of a 10 μm thick polymer membrane embedded in solid helium. A voltage applied to the membrane, which contained cylindrical channels with diameters of 6 to 8 μm, generated a pressure difference across the helium-filled channels. At high temperatures they observed thermally activated flow through channels, with activation energies between 6.5 and 13.9 K, consistent with vacancy activation energies in ^{4}He. Below 500 mK the temperature dependence is much weaker, corresponding flow activation energy around 0.5 K.

They attributed the high temperature flow to diffusion of thermally activated vacancies (Nabarro-Herring creep [31–34]) but the origin of the very slow creep at low temperature was unclear, although it might involve motion of dislocation kinks over their Peierls barrier.

Very recently, this group extended their flow measurements to bcc ^{3}He [23,35]. At high temperatures (above 200 mK) they saw thermally activated flow, with activation energies of 2.3–3.1 K, again comparable to thermal vacancy activation energies (e.g., 4.25 K at ~35 bar [36]) but much larger than the 0.85 K activation energy in our measurements. To compare flow rates, we converted our pressure change rates $\dot{P}$ to the average flow speeds shown on the right axis of Fig. 3, as described in the Supplemental Material [22]. In the thermally activated regime above 100 mK, our flow speeds were 3 to 4 orders of magnitude larger than those in Refs. [23,35]. There is a similar discrepancy in the low temperature nonthermal regime where the flow speeds in our experiments ($\sim 7 \times 10^{-8}$ cm/s) were also much larger than through the channels of their membrane ($\lesssim 10^{-10}$ cm/s), suggesting that different mechanisms must be responsible for the flow, despite the similar pressure differences in the two experiments.

Flow in solids involves the motion of defects—vacancies, dislocations, and grain boundaries. Vacancy diffusion, which is important at high temperatures, gives a flow rate proportional to the pressure gradient $(\Delta P/L)$, where L is the length of the flow channel. The maximum pressure differences in our measurements ($\Delta P \approx 70$ kPa) were similar to those used by Lisunov *et al.* (~6 kPa [35]). However, their channels were much shorter ($L = 10$ μm vs our cell's $L = 8.78$ mm) so their pressure gradients were much larger than ours (up to 600 kPa/mm vs 8 kPa/mm). Our vacancy flow velocities should therefore be 2 orders of magnitude *smaller*, but we see flow 3 to 4 orders of magnitude *larger*. This discrepancy of more than 5 orders of magnitude, and the fact that our activation energy of 0.85 K is much smaller than vacancy energies in ^{3}He, rule out vacancy diffusion as the direct source of flow in our experiments.

For solid ^{4}He in an open geometry, dislocations have been identified as the mechanism of plastic flow, including thermal creep at high temperatures [37]. The associated mass transfer is much more obvious than that caused by vacancy diffusion. The force on dislocations is proportional to the shear stress σ, not the pressure gradient. For a cylindrical channel with length L and diameter D, the maximum shear stress is $\sigma = (D/4L)\Delta P$ [38]. Since the aspect ratios (D/L) in the two sets of experiments are both of order 1, the maximum shear stress is our experiment (6.2 kPa) is about 6 times larger than in theirs (1 kPa). However, the deformation associated with each dislocation is proportional to the square of the distance between its pinning points and dislocations can be immobilized by impurities or narrow channels. At the stresses in these flow experiments, impurity (^{4}He) atoms are too weakly bound to pin dislocations, but they will be pinned at the walls of the 8 μm channels in the experiments of Lisunov *et al.* This limits dislocation motion, leaving vacancy diffusion as the only mass transport mechanism, which provides an explanation of the much smaller thermally activated flow and higher activation energy in their experiments.

Although small, the nonactivated flow rate at lowest temperature in Fig. 3 is $\sim 10^4$ times higher than in Refs. [23,35], which suggests that it also involves dislocation motions. Climbing of dislocations requires vacancies but gliding does not, so they remain mobile at very low stresses (below 1 mPa in hcp ^{4}He [39]) and temperatures (below 20 mK in bcc ^{3}He [20,40]). This implies the Peierls barrier in helium is extremely small, and possibly zero. The obvious candidate for nonthermal dislocation motion in these quantum solids is tunneling of kinks across the Peierls barrier. Kink-antikink pairs can be created, which then separate and propagate, allowing the dislocation to glide at a rate proportional to the kink tunneling frequency. This is analogous to the vacancy diffusion that would be expected if zero-point vacancies existed in helium. At high temperatures, the kink motion can also be thermally activated, increasing the dislocation's mobility and the associated flow rate.

Given our polycrystalline samples, grain boundaries could also play a role. For example, they could involve thin fluidlike layers whose viscosity might, in contrast to ^{4}He, increase at low temperatures and reduce the associated flow. However, we see flow that decreases exponentially at low temperatures, a much stronger dependence than that of ^{3}He's viscosity [41].

To summarize, we studied mass flow in a channel containing bcc ^{3}He, by mechanically compressing the solid at one end and measuring pressure response at the other end. This is the *same* method used in a previous experiment which showed an increasing flow in solid ^{4}He at low temperature [16]. We observed mass flow in bcc ^{3}He, but the flow rate *decreased* monotonically at low temperature, supporting the interpretation of previous experiments [13–16] in terms of superflow in solid ^{4}He. Above 100 mK we observed thermally activated flow but, rather than disappearing at lower temperatures, the flow approached a constant value, evidence of a nonthermal quantum flow mechanism. Although this is qualitatively similar to the flow seen in recent experiments involving flow of bcc ^{3}He confined in micron-scale channels [23,35], our flow rates were orders of magnitude larger in both the thermally activated and the quantum regimes. Together with our smaller activation energy, this indicates that dislocations, which would be pinned in micron-scale channels, are responsible for the large flows in the open geometry of our experiments. The flow we saw at temperatures as low as 30 mK suggests that kinks can be created and move along

dislocations by tunneling, as well as by thermal activation at higher temperatures.

This work was supported by a grant from NSERC Canada. Z. G. C. acknowledges the support from National Key R&D Program of China Grant No. 2018YFA0305604 and National Science Foundation of China (NSFC) Grant No. 11874403.

*zgcheng@iphy.ac.cn
†jbeamish@ualberta.ca

[1] A. F. Andreev and I. M. Lifshitz, Sov. Phys. JETP **29**, 1107 (1969).
[2] A. J. Leggett, Phys. Rev. Lett. **25**, 1543 (1970).
[3] G. Chester, Phys. Rev. A **2**, 256 (1970).
[4] E. Kim and M. H. W. Chan, Nature (London) **427**, 225 (2004).
[5] E. Kim and M. H. W. Chan, Science **305**, 1941 (2004).
[6] J. R. Beamish, A. D. Fefferman, A. Haziot, X. Rojas, and S. Balibar, Phys. Rev. B **85**, 180501 (2012).
[7] H. J. Maris, Phys. Rev. B **86**, 020502 (2012).
[8] D. Y. Kim and M. H. W. Chan, Phys. Rev. Lett. **109**, 155301 (2012).
[9] A. Eyal, X. Mi, A. V. Talanov, and J. D. Reppy, Proc. Natl. Acad. Sci. U.S.A. **113**, E3203 (2016).
[10] H. Choi, D. Takahashi, K. Kono, and E. Kim, Science **330**, 1512 (2010).
[11] J. Choi, T. Tsuiki, D. Takahashi, H. Choi, K. Kono, K. Shirahama, and E. Kim, Phys. Rev. B **98**, 014509 (2018).
[12] M. W. Ray and R. B. Hallock, Phys. Rev. Lett. **100**, 235301 (2008).
[13] Y. Vekhov, W. J. Mullin, and R. B. Hallock, Phys. Rev. Lett. **113**, 035302 (2014).
[14] J. Shin, D. Y. Kim, A. Haziot, and M. H. W. Chan, Phys. Rev. Lett. **118**, 235301 (2017).
[15] Z. G. Cheng, J. Beamish, A. D. Fefferman, F. Souris, S. Balibar, and V. Dauvois, Phys. Rev. Lett. **114**, 165301 (2015).
[16] Z. G. Cheng and J. Beamish, Phys. Rev. Lett. **117**, 025301 (2016).
[17] G. Agnolet, D. F. McQueeney, and J. D. Reppy, Phys. Rev. B **39**, 8934 (1989).
[18] D. D. Osheroff, R. C. Richardson, and D. M. Lee, Phys. Rev. Lett. **28**, 885 (1972).
[19] D. D. Osheroff, W. J. Gully, R. C. Richardson, and D. M. Lee, Phys. Rev. Lett. **29**, 920 (1972).
[20] Z. G. Cheng and J. Beamish, Phys. Rev. B **95**, 180103 (2017).
[21] Z. G. Cheng, F. Souris, and J. Beamish, J. Low Temp. Phys. **183**, 99 (2016).
[22] See Supplemental Material at http://link.aps.org/supplemental/10.1103/PhysRevLett.121.225304, which includes description of experimental cell, calculation of hydrostatic relaxation in solid sample, evaluation of thermal equilibrium between helium and the cell, estimate of applied pressure difference, pressure gradient and shear stress, estimate of flow velocity, and the phase data of ac measurements. The Supplemental Material includes Refs. [16,23–28].
[23] A. Lisunov, V. Maidanov, V. Rubanskyi, S. Rubets, E. Rudavskii, S. Smirnov, and V. Zhuchkov, Phys. Rev. B **92**, 140505 (2015).
[24] R. Wanner, Phys. Rev. A **3**, 448 (1971).
[25] R. L. Rusby, M. Durieux, A. L. Reesink, R. P. Hudson, G. Schuster, M. Kühne, W. E. Fogle, R. J. Soulen, and E. D. Adams, J. Low Temp. Phys. **126**, 633 (2002).
[26] D. S. Greywall, Phys. Rev. B **15**, 2604 (1977).
[27] F. Pobell, *Matter and Methods at Low Temperatures* (Springer-Verlag, Berlin Heidelberg, 2007).
[28] P. F. Sullivan and G. Seidel, Phys. Rev. **173**, 679 (1968).
[29] J. Day and J. Beamish, J. Low Temp. Phys. **148**, 683 (2007).
[30] V. A. Zhuchkov, A. A. Lisunov, V. A. Maidanov, A. S. Neoneta, V. Y. Rubanskyi, S. P. Rubets, E. Y. Rudavskii, and S. N. Smirnov, Low Temp. Phys. **41**, 169 (2015).
[31] C. Herring, J. Appl. Phys. **21**, 437 (1950).
[32] J. R. Beamish, N. Mulders, A. Hikata, and C. Elbaum, Phys. Rev. B **44**, 9314 (1991).
[33] D. J. Sanders, H. Kwun, A. Hikata, and C. Elbaum, Phys. Rev. Lett. **39**, 815 (1977).
[34] D. J. Sanders, H. Kwun, A. Hikata, and C. Elbaum, Phys. Rev. Lett. **40**, 458 (1978).
[35] A. Lisunov, V. Maidanov, V. Rubanskyi, S. Rubets, E. Rudavskii, and S. Smirnov, Low Temp. Phys. **42**, 1075 (2016).
[36] S. M. Heald, D. R. Baer, and R. O. Simmons, Phys. Rev. B **30**, 2531 (1984).
[37] Z. G. Cheng and J. Beamish, Phys. Rev. Lett. **121**, 055301 (2018).
[38] A. Suhel and J. R. Beamish, Phys. Rev. B **84**, 094512 (2011).
[39] A. Haziot, X. Rojas, A. D. Fefferman, J. R. Beamish, and S. Balibar, Phys. Rev. Lett. **110**, 035301 (2013).
[40] O. Syshchenko and J. Beamish, J Phys. Conf. Ser. **150**, 032100 (2009).
[41] M. A. Black, H. E. Hall, and K. Thompson, J. Phys. C **4**, 129 (1971).